Office of Naval Research
DEPARTMENT OF THE NAVY
Contract N6onr-24420 (NR 062-059)

A note on the LINEAR AND NONLINEAR THEORIES for FULLY CAVITATED HYDROFOILS

T. Yao-tsu Wu

Hydrodynamics Laboratory
CALIFORNIA INSTITUTE OF TECHNOLOGY
Pasadena, California

Report No. 21-22
August 1956

Approved by:
M. S. Plesset

Office of Naval Research
Department of the Navy
Contract N6onr-24420 (NR 062-059)

A NOTE ON THE LINEAR AND NONLINEAR THEORIES FOR FULLY CAVITATED HYDROFOILS

T. Yao-tsu Wu

Hydrodynamics Laboratory
California Institute of Technology
Pasadena, California

Report No. 21-22
August, 1956

Approved:
M. S. Plesset

LIST OF SYMBOLS

(x, y) - the rectangular coordinates, $z = x + iy$ see Fig. 1

$\eta(x)$ - the lower surface camber of a hydrofoil

α - angle of attack of the hydrofoil

U - uniform flow velocity at infinity

$\vec{q}$ - velocity vector of the flow

p - pressure; P, the pressure at infinity

p_c - the pressure in the cavity, a constant

ρ - the liquid density, a constant

σ - the cavitation number, $= (P - p_c)/(\frac{1}{2} \rho U^2)$

q_c - a constant velocity on the cavity boundary

(u, v) - perturbation velocity based on q_c : $\vec{q}/q_c = (1 + u, v)$

(u_1, v_1) - perturbation velocity based on U : $\vec{q}/U = (1 + u_1, v_1)$

w - the complex velocity, $w(z) = u - i v$

β - a constant, $= 1 - (1 + \sigma)^{-1/2}$

ℓ - the ratio of the cavity length and the chord

C_p - the pressure coefficient based on p_c, $= (p - p_c)/(\frac{1}{2} \rho U^2)$

ν, ζ - two complex planes

a - a quantity defined by $a = \sqrt{\ell - 1}$

A, B, c_o, c_n - constants and coefficients

$\delta, \epsilon, \lambda, \tau$ - quantities defined by $\delta = \left[\sqrt{1 + a^2} + 1\right]^{1/2}$, $\epsilon = \left[\sqrt{1 + a^2} - 1\right]^{1/2}$,

$$\lambda = \sqrt{a}\,(\delta - \epsilon) - 1, \qquad \tau = \sqrt{a}\,(\delta + \epsilon) - 2a$$

C_L, C_D - the lift and drag coefficient

γ - half of the arc angle of a circular arc profile

INTRODUCTION

The lifting problem of fully cavitated hydrofoils has recently received some attention. The nonlinear problem of two-dimensional fully cavitated hydrofoils has been treated by the author,[1] using a generalized free streamline theory. The hydrofoils investigated in Ref. 1 were those with sharp leading and trailing edges which are assumed to be the separation points of the cavity streamlines. Except for this limitation, the nonlinear theory is applicable to hydrofoils of arbitrary geometric profile, operating at any cavitation number, and for almost all angles of attack as long as the cavity wake is fully developed. By using an elegant linear theory, Tulin[2] has treated the problem of a fully cavitated flat plate set at a small angle of attack and operated at arbitrary cavitation number. In the case of hydrofoils of arbitrary profile operating at zero cavitation number, some interesting simple relationships are given by Tulin for the connection between the lift, drag and moment of a supercavitating hydrofoil and the lift, moment and the third moment of an equivalent airfoil (unstalled).

In the present investigation, Tulin's linear theory is first extended to calculate the hydrodynamic lift and drag on a fully cavitated hydrofoil of arbitrary camber at arbitrary cavitation number. A numerical example is given for a circular hydrofoil subtending an arc angle of 16°, for which the corresponding nonlinear solution is available.[1] A direct comparison between these two theories is made explicitly for the flat plate and the circular arc hydrofoil. Some important aspects of the results are discussed subsequently.

FORMULATION OF THE LINEARIZED THEORY

Consider a two-dimensional lifting surface with sharp leading and trailing edges, its lower surface has a small arbitrary camber given by $\eta(x)$, and its chord length is unity (see Fig. 1). When this

lifting foil (or hydrofoil) is held at a small, positive attack angle α to a stream of liquid which fills a space of infinite extent and has a uniform constant velocity U at infinity, the resulting flow velocity of the liquid will be denoted by $\vec{q}$. If the velocity $\vec{q}$ is known, the pressure field p for steady motion can be calculated from the Bernoulli equation

$$p + \frac{1}{2}\rho q^2 = P + \frac{1}{2}\rho U^2 \tag{1}$$

where P is the pressure at infinity, and ρ is the liquid density taken to be constant. When the velocity U is sufficiently large so that the local pressure on the suction side of the hydrofoil becomes less than the vapor pressure p_c of the liquid, the liquid boils locally to form an integral cavity. The general character of such cavity flows depends on the value of the cavitation number:

$$\sigma = (P - p_c)/(\tfrac{1}{2}\rho U^2) \ . \tag{2}$$

This paper is concerned in particular with the hydrofoils fully cavitated at such low cavitation numbers that the trailing cavities extend beyond the trailing edge. After the cavity is fully developed, the small thickness of the hydrofoil has no effect on the flow and, therefore, only the ordinates of the lower surface matter. A typical flow configuration is shown in Fig. 1. Inside the cavity, which is filled with vapor or a vapor-gas mixture, the pressure is assumed to be constant and is denoted by p_c. Consequently the cavity boundary, a free surface, is a surface of constant velocity, on which $q \equiv |\vec{q}| = q_c$, say. By using Eqs. (1) and (2), the value of q_c is found to be

$$q_c = U\sqrt{1+\sigma} \ . \tag{3}$$

Apparently, q_c is a characteristic value of the flow velocity near the cavity, just as U is for the flow at infinity. It is convenient here to take q_c as the reference velocity; the velocity of the liquid flow

may then be written as*

$$\vec{q}/q_c = (1+u, v) \tag{4}$$

so that (u, v) represents the nondimensional perturbation velocity due to the presence of the hydrofoil and the cavity wake. Outside the cavity, the flow is assumed to be incompressible and irrotational so that (u, v) are governed by the continuity equation

$$\frac{\partial u}{\partial x} = -\frac{\partial v}{\partial y} \tag{5}$$

and the condition of irrotationality

$$\frac{\partial u}{\partial y} = \frac{\partial v}{\partial x} \ . \tag{6}$$

Equations (5) and (6) imply that the complex velocity $w = u - iv$ must be an analytic function of the complex variable $z = x+iy$ where (x, y) are the rectangular coordinates in the flow plane (see Fig. 1), or

$$w(z) = u - iv \ . \tag{7}$$

The boundary conditions of this problem can be determined as follows. At infinity, $\vec{q} = (U, 0)$; hence, from Eqs. (3) and (4), we have

$$u = -\left[1-(1+\sigma)^{-1/2}\right] \equiv -\beta \qquad \text{and} \qquad v = 0 \quad \text{at} \quad z = \infty. \tag{8}$$

---

*Of course, U may be equally suitable for a reference velocity so that $\vec{q}/U = (1+u_1, v_1)$. However, since near the cavity the numerical value of u is appreciably less than that of u_1 for $\sigma > 0$, the use of (u, v) gives a more straightforward approximation of the boundary conditions. Furthermore, these two reference systems result in slightly different expressions, even in the linear term, for the pressure coefficient on the body. Details are given in Appendix I.

This condition is exact. In order to simplify the boundary conditions on the cavity boundary and the wetted lower surface of the hydrofoil, we assume that both the camber $\eta(x)$ and the attack angle α are small quantities of the first order. Squares and higher powers of these quantities will be neglected. Under this condition, the cavity, which starts from the leading edge A (see Fig. 1) and extends beyond the trailing edge B for small enough σ, should have a long and narrow configuration. Furthermore, it is reasonable to assume that, except for the gravitational effect*, the cavity is approximately aligned in the undisturbed flow direction and thus ends up at point C on the x-axis where $x_c = \ell\,(>1)$. Note that ℓ is as yet unknown and must be solved for as a part of the problem. On the cavity boundary, $|\vec{q}| = q_c$, or $(1+u)^2 + v^2 = 1$; hence to the first order, $u = 0$. Subject to an error of the order already neglected, this condition may be applied on the x-axis. Therefore,

$$u = 0 \qquad \text{for} \qquad 0 < x < \ell\,, \qquad y = 0+\;;$$

$$u = 0 \qquad \text{for} \qquad 1 < x < \ell\,, \qquad y = 0-\;. \tag{9}$$

On the wetted lower surface of the hydrofoil, the flow must be tangential to the solid surface, or, with $v/(1+u)$ linearized to v,

$$v = -\alpha + \frac{d\eta}{dx} \qquad \text{for} \qquad 0 < x < 1\,, \qquad y = 0-\;. \tag{10}$$

These boundary conditions (8)-(10) are shown in Fig. 2. The fourth boundary condition, which is the same as the Kutta condition in airfoil theory, is that the velocity must be finite in the neighborhood of the trailing edge. There is another condition, which may be called the closure condition, that the cavity boundary together with the wetted surface must form a closed contour. This condition may be expressed mathematically as

---

*The gravitational effect on the fully cavitating flow over a hydrofoil is discussed by B. R. Parkin (Ref. 3).

$$\mathrm{Im} \oint_{\Gamma} w(z)\, dz = 0 \tag{11}$$

where the closed contour Γ consists of the cavity boundary and the wetted surface, and may, of course, be deformed to any closed contour within the liquid enclosing the cavity since $w(z)$ is regular there. This closure condition (11) is analogous to one used in thin airfoil theory that, when the airfoil is represented by a distribution of singularities, a singularity of the source type must be excluded. Note, however, that unlike the case of the thin airfoil (or the pure drag case) for which u (or v) can be prescribed (namely, zero) on the x-axis off the body, the value of u or v may not be specified in this problem for $x<0$ or $x>\ell$ on $y=0$, but must be determined from the solution.

With respect to the cavity pressure p_c, the pressure coefficient defined by $(p-p_c)/(\frac{1}{2}\rho U^2)$ can be expressed in terms of velocity by using the linearized version of Eq. (1),

$$p + \frac{1}{2}\rho q_c^2 (1+2u) = p_c + \frac{1}{2}\rho q_c^2$$

to yield

$$C_p \equiv \frac{p-p_c}{\frac{1}{2}\rho U^2} \cong -(1+\sigma)(2u) \ . \tag{12}$$

It can be seen that the linearized condition (10) and the linearized expression for C_p, Eq. (12), break down near the stagnation point (where $u=-1$, $v=0$), that is, in the neighborhood of the leading edge where x is of the order of a^2.

It should be pointed out that the streamline at the rear end of the cavity, separating the flow from a region of constant pressure, has a branch point at C. Consequently $w(z)$ has a certain singular behavior at $z=\ell$. Such a potential problem is well known (e.g. see Ref. 4), and it can be shown that this singularity behaves like

$$w(z) = K(z-\ell)^{-1/2} \qquad \text{near} \quad z=\ell \ , \tag{13}$$

where K is a constant. A remark should be made that, when this problem was solved in its original nonlinear form, an appropriate potential model has to be introduced to give a good approximation of the flow in the cavity wake, as was commented upon in Ref. 1. In the present linearized formulation, however, no model is really necessary to represent the flow in the cavity wake; only the singular behavior given by Eq. (13) is essential.

Since no boundary condition is prescribed on the x-axis outside the section $0 < x < \ell$, the determination of $w(z)$ may proceed by applying the conformal transformation

$$\nu = e^{i\pi} \left[(\ell - 1) \frac{z}{\ell - z} \right]^{1/2} \tag{14}$$

which maps the original plane on to the lower half of the ν-plane; the wetted surface maps on to $0 \leq R\ell\nu \leq 1$ and the cavity boundary corresponds to the rest of the real ν-axis. The point $z = \infty$ is now at

$$\nu_{(z=\infty)} = -i\sqrt{\ell - 1} \equiv -ia \ . \tag{15}$$

Transformation (14) becomes singular as $\ell \to 1$, implying that the present linear theory is not likely to be much good for ℓ too close to unity. The range of validity of the linear theory will be investigated later when the solution is obtained.

Next we introduce the Joukowsky transformation

$$\nu = \frac{(\zeta+1)^2}{4\zeta} \tag{16}$$

which maps the wetted surface on to the lower half of the unit circle $|\zeta| = 1$, the cavity boundary being still on the real ζ-axis outside the unit circle. Throughout these mappings the value of w is kept invariant

at all image points so that the boundary conditions in different planes are as shown in Fig. 2.

Thus, in the ν-plane, $u=0$ on $\mathrm{Im}\,\nu=0$ for $\mathrm{Re}\,\nu<0$ and $\mathrm{Re}\,\nu>1$. It follows that $w(\nu)$ can be continued analytically into the upper half plane by Schwarz's principle of reflection:

$$w(\overline{\nu}) = -\overline{w}(\nu) \tag{17}$$

so that u is odd and v is even in $\mathrm{Im}\,\nu$. Obviously the same argument holds for w in the ζ-plane. Therefore, on the unit circle $\zeta = e^{i\theta}$, we may expand the boundary condition into a cosine series of θ; that is,

$$\frac{d\eta}{dx} = c_o + \sum_{n=1}^{\infty} c_n \cos n\theta \qquad (\zeta = e^{i\theta}) \tag{18a}$$

where

$$c_o = \frac{1}{\pi}\int_o^{\pi} \frac{d\eta}{dx}\, d\theta\,, \qquad c_n = \frac{2}{\pi}\int_o^{\pi} \frac{d\eta}{dx} \cos n\theta\, d\theta \quad (n=1, 2\ldots)\,. \tag{18b}$$

From Eqs. (14) and (16), it may be verified that x and θ in Eq. (18b) are related by

$$x = (1+a^2)\cos^4\frac{\theta}{2}\left[\cos^4\frac{\theta}{2} + a^2\right]^{-1}, \qquad (a = \sqrt{\ell - 1})\,. \tag{18c}$$

Consequently, condition (10) becomes

$$v = (c_o - a) + \sum_{1}^{\infty} c_n \cos n\theta \qquad \text{on} \quad \zeta = e^{i\theta}\,. \tag{19}$$

In a strict sense, the coefficients c_o and c_n are as yet unknown since ℓ in Eq. (18c) has to be determined.

The general behavior of w and the type and location of its singularities may be easily ascertained in the ζ-plane. The function $w(\zeta)$ must satisfy the following conditions:

(a) $w(\zeta)$ is regular everywhere for $|<|\zeta|<\infty$;

(b) it follows from Eq. (13) that, except for a proportionality constant, $w(\zeta) \sim \zeta$ near $\zeta = \infty$ and hence for $|\zeta| > 1$, $w(\zeta)$ may be expanded into a descending power series in ζ beginning with the term ζ ;

(c) $R\ell\ w = 0$ on the real ζ-axis for $R\ell\ \zeta < -1$ and $R\ell\ \zeta > 1$;

(d) at the leading edge, $\zeta = -1$, $w(\zeta) \sim (\zeta+1)^{-1}$, a well-known type of singularity that appears in thin airfoil theory (Ref. 5);

(e) near the trailing edge, $\zeta = 1$, w is continuous and hence $R\ w = 0$ at $\zeta = 1$;

(f) $v = -\mathrm{Im}\ w$ satisfies Eq. (19) on $|\zeta| = 1$.

Therefore $w(\zeta)$ must be of the form

$$w(\zeta) = i\,\frac{A}{4}\left(\zeta - \frac{1}{\zeta}\right) + iB\,\frac{\zeta-1}{\zeta+1} - i\left[(c_o - a) + \sum_1^\infty c_n\,\zeta^{-n}\right] \qquad (20)$$

where A, B are real arbitrary constants and c_o, c_n are given by Eq. (18). This expression for w obviously fulfills the conditions (a) to (e). To verify that the condition (f) is satisfied, we note that on $\zeta = e^{i\theta}$,

$$w = u - iv = -\frac{A}{2}\sin\theta - B\tan\frac{\theta}{2} - i\left[(c_o - a) + \sum_1^\infty c_n(\cos n\theta - i\sin\theta)\right]$$

so that v satisfies Eq. (19). Upon transformation of Eq. (20) back to the ν-plane, $w(\nu)$ takes the form:

$$w(\nu) = i\,\sqrt{\nu-1}\left(A\sqrt{\nu} + \frac{B}{\sqrt{\nu}}\right) - i\left[(c_o - a) + \sum_1^\infty c_n\,\zeta^{-n}\right] \qquad (21a)$$

where

$$\left[\zeta(\nu)\right]^{-1} = (2\nu - 1) - 2\sqrt{\nu(\nu-1)}\ . \qquad (21b)$$

Now conditions (8) and (11) can be applied to determine the constants A, B, ℓ and hence c_o and c_n. At $z = \infty$, or $\nu = -ia$

(see Eq. 15),

$$\sqrt{\nu} = \sqrt{a}\, e^{-i\pi/4} , \qquad \sqrt{\nu-1} = \frac{1}{\sqrt{2}} (\epsilon - i\delta) , \tag{22a}$$

with

$$\delta = \left[\sqrt{1+a^2} + 1\right]^{1/2} , \qquad \epsilon = \left[\sqrt{1+a^2} - 1\right]^{1/2} . \tag{22b}$$

Also, at $\nu = -ia$, the term ζ^{-1} in Eq. (21) assumes the value

$$\zeta_E^{-1} = \lambda + i\tau \tag{23a}$$

with

$$\lambda = \sqrt{a}\,(\delta - \epsilon) - 1 , \qquad \tau = \sqrt{a}\,(\delta + \epsilon) - 2a \tag{23b}$$

It can be shown that its modulus $\left|\zeta_E^{-1}\right| = (\lambda^2+\tau^2)^{1/2}$ decreases monotonically and rapidly from unity at $a=0$ to zero at $a=\infty$. (At $a=1$, $\left|\zeta_E^{-1}\right| \doteq 0.22$). Thus, within the framework of the linear theory, the terms c_3, c_4, ... in Eqs. (18) to (21) may be neglected. Substituting Eqs. (22) and (23) into (21) and using condition (8), we obtain

$$\sqrt{a}\, A = \frac{1}{2\sqrt{1+a^2}} \left[(\delta - \epsilon)\,\alpha' - (\delta+\epsilon)\,\beta'\right] , \tag{24a}$$

$$B/\sqrt{a} = -\frac{1}{2\sqrt{1+a^2}} \left[(\delta+\epsilon)\,\alpha' + (\delta-\epsilon)\,\beta'\right] , \tag{24b}$$

where

$$\alpha' = \alpha - c_o - c_1\lambda + c_2(\tau^2 - \lambda^2) , \qquad \beta' = \beta + \tau\,(c_1 + 2c_2\lambda) . \tag{24c}$$

Finally, condition (11) is applied to determine a in terms of known physical quantities α, σ and $\eta(x)$. Let us consider the integral

$$I = \oint_\Gamma w(z)\,dz = a^2(1+a^2)\int_{-\infty-ib}^{\infty-ib} \frac{dw}{d\nu}\,\frac{d\nu}{(\nu^2+a^2)}\,, \tag{25}$$

where $0 < b < a$ and $w(\nu)$ is given by Eq. (21), the last integral being obtained by integration by parts. In the lower half of the ν-plane $dw/d\nu$ is a one-valued function of ν, regular everywhere, and is of the order unity as $\nu \to \infty$; while the term $(\nu^2+a^2)^{-1}$ in the integrand has a simple pole at $\nu = -ia$. Hence by applying the theorem of residues, we obtain

$$I = \pi a(1+a^2)\,(dw/d\nu)_{\nu=-ia}$$

$$= \frac{\pi}{2} ia(1+a^2)\left\{\frac{A(2\nu-1) + B\nu^{-1} + 2c_1\zeta^{-1} + 4c_2\zeta^{-2}}{\sqrt{\nu(\nu-1)}}\right\}_{\nu=-ia}. \tag{26}$$

Substituting Eqs. (22) and (23) into (26) and using relations (24), one can verify, after some manipulation, that

$$I = -\frac{\pi}{4}(\delta-\epsilon)^2\left[\beta + a(\alpha-c_o) + G\right] + i\frac{\pi}{4}(\delta+\epsilon)^2\left[(\alpha-c_o) - a\beta + H\right] \tag{27}$$

with

$$G = -a(c_1+c_2) + 8a(1+a^2)c_2\left[1 - (\delta+\epsilon)^2\tau\right],$$

$$H = (a^2c_1 - c_2) - (1+a^2)\left\{c_1\left[2a(\delta-\epsilon)^2 - 1\right] + 8ac_2(\delta-\epsilon)^2\lambda\right\}.$$

Since condition (11) requires that Im $I = 0$,

$$a\beta = \alpha - c_o + H \tag{28}$$

where β is defined in Eq. (8). This result obtained from the closure condition determines β, and hence the cavitation number σ,

parametrically in terms of a. It then follows that the integral I is purely real,

$$I = -\frac{\pi}{2}\left(\sqrt{1+a^2} - a\right)\left[\frac{1+a^2}{a}\left(\alpha - c_o\right) + G + H/a\right] \quad . \tag{29}$$

Now the lift coefficient C_L can be calculated by using Eq. (12),

$$C_L = \frac{L}{\frac{1}{2}\rho U^2} = \oint C_p\, dz = -2(1+\sigma)\oint u\, dz = -2(1+\sigma)\, I \tag{30}$$

since $\mathrm{Im}\, I = 0$. After some simplification, we obtain

$$C_L = \pi(1+\sigma)\left(\sqrt{1+a^2} - a\right)\frac{(1+a^2)}{a}\left\{\alpha - c_o - c_1\left[2a(\delta-\epsilon)^2 - 1\right]\right.$$

$$\left. + c_2\left[8a^2 - 1 - 8a^2\tau(\delta+\epsilon)^2 - 8a\lambda(\delta-\epsilon)^2\right]\right\} \quad . \tag{31}$$

The drag coefficient is given by the following integral:

$$C_D = \frac{D}{\frac{1}{2}\rho U^2} = -\int_o^1 v\, C_p\, dz = 2(1+\sigma)\int_o^1 u\, v\, \frac{dz}{d\nu}\, d\nu \tag{32}$$

where the integration is taken on $\mathrm{Im}\ \nu = 0-$ for $0 \le R\ell\ \nu \le 1$. Thus, on the path of integration, we take $\sqrt{\nu - 1} = \sqrt{1-\nu}\, \exp(-i\pi/2)$; and consequently $w(\nu) = u(\nu) - i\, v(\nu)$ assumes there the following value:

$$u(\nu) = \sqrt{\nu(1-\nu)}\left[(A + 2c_1 - 4c_2) + B/\nu + 8c_2\nu\right] \tag{33a}$$

$$v(\nu) = (c_o - \alpha - c_1 + c_2) + 2c_1\nu - 8c_2\nu(1-\nu) \quad . \tag{33b}$$

Substituting Eq. (33) into Eq. (32), we obtain

$$C_D = (\alpha - c_o + c_1 - c_2)\, C_L + 4(1+\sigma)\int_o^1 u(\nu)\left[c_1 - 4c_2(1-\nu)\right]\nu\, \frac{dz}{d\nu}\, d\nu \quad ,$$

where in the first term the use is made of Eq. (30). Upon integration by parts and introduction of the new variable θ, defined by $\nu = \cos^2 \frac{\theta}{2}$, the above integral may be expressed in terms of a linear combination of the integrals of the form

$$J_n = \frac{1}{\pi}\int_0^{\pi} \frac{\cos n\theta \, d\theta}{a^2 + \cos^4(\theta/2)} = R\ell \, \frac{\left[(\delta+\epsilon)+i(\delta-\epsilon)\right]\left[\lambda+i\tau\right]^n}{2a^{3/2}(1+a^2)^{1/2}} , \qquad (34)$$

where $n = 0, 1, 2, \ldots$ and δ, ϵ, λ, τ are given by Eq. (22b) and (23b)*. After some manipulation and rearrangement of the terms, one may verify that

$$C_D = \pi(1+\sigma)(\sqrt{1+a^2} - a)\frac{(1+a^2)}{a}\left\{\alpha - c_o - \frac{c_1}{2}\left[2a(\delta-\epsilon)^2 - 1\right]\right\}^2 . \qquad (35)$$

Equations (31) and (35) together with (28) give the parametric expression for C_L and C_D in terms of the parameter a. If a specific profile $\eta(x)$ and its attack angle α are given, the numerical computation of C_L and C_D can be carried out as follows. We first assign a value (positive) to the parameter a, the relation $x = x(\theta)$ given by Eq. (18c) is then fixed so that the coefficients c_o and c_n can be calculated from Eq. (18b). Next, the cavitation number σ of this specific flow can be determined from Eq. (28); the calculation of C_L and C_D then becomes straightforward.

It should be noted that in the present linear theory only α and the camber functions c_o and c_n are taken to be small, while the parameter a and hence the cavitation number σ are so far left arbitrary. However, it follows from Eq. (28) that for given α and $\eta(x)$ (and hence c_n's), the value of a is limited to the range which can be expressed implicitly by

$$\alpha - c_o + H \leq a \qquad (36)$$

---

*The evaluation of this integral is given in Appendix II.

since $\beta \leq 1$. For practical application, the range of a for the theory to hold is to be discussed later when the explicit solution is computed. Though it is obvious (as was already explained before, following Eq. (15)) that the linear theory breaks down as $a \to 0$ ($\ell \to 1$), the present solution is expected to be valid for $a > 1$ ($\ell > 2$). For very large values of a, the solution may be expanded into the following form: Equation (28) becomes

$$a\beta \cong (\alpha - c_o - \frac{c_1}{2}) + \frac{1}{4a^2}\left[c_1(1 - \frac{3}{8a^2}) + \frac{5}{4}\, c_2(1 - \frac{5}{8a^2}) + 0(a^{-4})\right], \tag{37a}$$

or,

$$\sigma \cong \frac{2}{a}\left[(\alpha - c_o - \frac{c_1}{2}) + \frac{c_1}{4a^2} + \frac{5c_2}{16a^2}\right]\left[1 + \frac{3}{2a}(\alpha - c_o - \frac{c_1}{2}) + 0(\frac{a}{a})^2\right], \tag{37b}$$

and

$$C_L \cong \frac{\pi}{2}(1+\sigma)\left\{(\alpha - c_o - c_1 - \frac{c_2}{2}) + \frac{3}{4a^2}(\alpha - c_o - \frac{c_1}{3} + \frac{7}{12}\, c_2) + o(\frac{a}{a^2})\right\}, \tag{38}$$

$$C_D \cong \frac{\pi}{2}(1+\sigma)(\alpha - c_o - \frac{c_1}{2})\left\{(\alpha - c_o - \frac{c_1}{2}) + \frac{3}{4a^2}(\alpha - c_o + \frac{c_1}{6}) + o(\frac{a}{a^2})\right\}. \tag{39}$$

From these results one may easily deduce the asymptotic value of the cavity length for $a \gg 1$ (or $\sigma \ll 1$) as:

$$\ell \sim a^2 \sim \frac{8\, C_D}{\pi \sigma^2}\left[1 + 0(\sigma)\right] \tag{40}$$

which is a general feature of cavity flows at small cavitation numbers (e.g., see Ref. 2, p. 2).

SPECIAL CASES

The following special cases are of primary interest.

(A) The limiting case of $\sigma = 0$.

From Eq. (37) we see that $\sigma \to 0$ as $a \to \infty$. In this limit, the cavity is then infinitely long (see Eq. 40); and Eq. (18c) becomes

$$x = \cos^4 (\theta/2) \tag{41}$$

which leads to direct determination of c_o and c_n. The corresponding limits of C_L and C_D are

$$C_L = \frac{\pi}{2} \left(a - c_o - c_1 - \frac{c_2}{2}\right) , \qquad C_D = \frac{\pi}{2} \left(a - c_o - \frac{c_1}{2}\right)^2 . \tag{42}$$

This result, first obtained by Tulin[2], agrees reasonably well with the corresponding limit $(\sigma \to 0)$ of the nonlinear solution.[1] For example, we take the circular arc profile subtending a small arc angle 2γ , or

$$\eta(x) = \gamma x(1 - x) \qquad \text{for} \qquad 0 \le x \le 1 . \tag{43}$$

Then

$$\frac{d\eta}{dx} = \gamma(1 - 2\cos^4 \frac{\theta}{2}) = \frac{\gamma}{4} - \gamma \cos\theta - \frac{\gamma}{4} \cos 2\theta .$$

Comparison of this expression with Eq. (18a) shows that

$$c_o = \gamma/4 , \qquad c_1 = -\gamma , \qquad c_2 = -\gamma/4 . \tag{44}$$

Hence

$$C_L = \frac{\pi}{2}(a + \frac{7}{8}\gamma) , \qquad C_D = \frac{\pi}{2} (a + \frac{\gamma}{4})^2 ; \tag{45}$$

and

$$\frac{\partial C_L}{\partial \gamma} = \frac{7\pi}{16}, \qquad \frac{\partial C_D}{\partial \gamma} = \frac{\pi}{4}\left(\alpha + \frac{\gamma}{4}\right). \tag{46}$$

This particular result agrees with the corresponding limit of the nonlinear solution (see Ref. 1, Eq. 4.31).

(B) The flat plate hydrofoil at arbitrary σ.

For the flat plate, $\eta(x) = 0$, and hence c_o and c_n all vanish. Then Eq. (28) becomes

$$a\beta = \alpha \qquad \text{or} \qquad a \equiv \sqrt{\ell - 1} = \frac{\alpha\sqrt{1+\sigma}}{\sqrt{1+\sigma} - 1}\ ; \tag{47}$$

and the value of C_L and C_D are now

$$C_L = \pi\alpha(1+\sigma)\left(\sqrt{1+a^2} - a\right)\frac{1+a^2}{a}, \qquad C_D = \alpha C_L. \tag{48}$$

When $\beta/\alpha = \left[1 - (1+\sigma)^{-1/2}\right]/\alpha$ is plotted against $1/\ell$ we obtain a curve as shown in Fig. 3. The value of C_L given by Eq. (48) is plotted versus σ in Fig. 4 for several small attack angles. This linear result of C_L and C_D are further compared with the nonlinear solution of Ref. 1 as shown in Figs. 5 and 6.

(C) The circular arc hydrofoil at arbitrary σ.

Again we take the circular arc profile given by Eq. (43) so that

$$d\eta/dx = \gamma(1 - 2x) \tag{49}$$

where the function $x(\theta)$ is given by Eq. (18c). In the evaluation of the coefficients c_o, c_1, and c_2, use may be made of the integrals J_n given by Eq. (34) to yield

$$c_o = \gamma\left\{2a^2(1+a^2)\,J_o - 1 - 2a^2\right\} = \gamma\left\{(\delta+\epsilon)\sqrt{a(1+a^2)} - 1 - 2a^2\right\},$$

$$c_1 = 4\gamma a^2(1+a^2)\, J_1 = -\gamma \sqrt{a(1+a^2)}\ (\delta - \epsilon)^3 \ , \tag{50}$$

$$c_2 = 4\gamma\, a^2(1+a^2)\, J_2 = -\,2\gamma \left[8a\tau(1+a^2) - (\delta+\epsilon)\sqrt{a(1+a^2)}\right] \ .$$

Thus in this case, Eqs. (50), (28), (31) and (35) form the complete solution.

For very small σ ($a \gg 1$), one may expand the above expressions into the form

$$c_o \cong \frac{\gamma}{4}\left[1 - \frac{13}{16a^2} + \frac{49}{128a^4} + O(a^{-6})\right] \ ,$$

$$c_1 \cong -\gamma\left[1 + \frac{1}{8a^2} - \frac{13}{128a^4} + O(a^{-6})\right] \ , \tag{51}$$

$$c_2 \cong -\frac{\gamma}{4}\left[1 - \frac{3}{4a^2} + O(a^{-4})\right] \ .$$

Equations (37)-(39) then simplify to

$$a\beta \cong \alpha + \frac{\gamma}{4}\left[1 - \frac{1}{4a^2} + \frac{3}{32a^4} + O(a^{-6})\right] \ , \tag{52a}$$

or,

$$\sigma \cong \frac{2}{a}\left[(\alpha + \tfrac{\gamma}{4}) + \frac{3}{2a}(\alpha + \tfrac{\gamma}{4})^2 - \frac{\gamma}{16a^2} + O\left(\frac{a^2}{a^3}, \frac{\gamma}{a^4}\right)\right] \ , \tag{52b}$$

$$C_L \cong \frac{\pi}{2}(1+\sigma)\left[\alpha + \frac{7\gamma}{8} + \frac{3}{4a^2}(\alpha + \tfrac{\gamma}{4}) + O\left(\tfrac{\alpha}{a}\right)^2\right] \ , \tag{53}$$

$$C_D \cong \frac{\pi}{2}(1+\sigma)(\alpha + \tfrac{\gamma}{4})\left[(\alpha + \tfrac{\gamma}{4}) + \frac{3}{4a^2}(\alpha + \tfrac{7\gamma}{24}) + O\left(\tfrac{\alpha}{a}\right)^2\right] . \tag{54}$$

These asymptotic formulas give a good approximation to C_L and C_D for $a \geq 2$. At $a = 2$, the error committed by neglecting the order terms in the above equations is less than 3%; while for $a < 2$, Eqs. (31) and (35) should be used. The values of C_L and C_D for $\gamma = 8^o$ are plotted against σ in Figs. 7 and 8 respectively; their comparison with the nonlinear solution[1] is shown in Figs. 9 and 10. The quantity $\left[1 - (1+\sigma)^{-1/2}\right]/\alpha$ for $\gamma = 8^o$ is plotted versus $1/\ell$ in Fig. 3 for several small angles of attack.

DISCUSSION AND COMPARISON OF THE LINEAR AND NONLINEAR THEORIES

In the present linear theory, the linearization is, strictly speaking, imposed only on α and c_n's, while the parameter $a\,(= \sqrt{\ell - 1})$, being subject only to the condition (36), is otherwise left arbitrary. In fact, a appears in the solution in a quite complicated way. One important feature, however, may be seen from Fig. 3. For given α, the cavity length decreases monotonically with increasing σ; the effect of camber merely produces a longer cavity, for the same α and σ, than the flat plate case. When applied to the flat plate hydrofoil, condition (36) becomes

$$a \geq \alpha \qquad \text{or} \qquad \ell \geq 1 + \alpha^2 .$$

Hence $\ell = 1$ $(a = 0)$ is impossible in this case unless $\alpha = 0$. Likewise one may find a lower bound $a_m (> 0)$ of a for the circular arc hydrofoil. Though in general the limit $\ell = 1$ cannot be reached, $(\ell - 1)$ may become very small (of the order α^2) under certain circumstances. The smaller the quantity $(\ell - 1)$, the poorer the linear approximation, because, literally speaking, as $\ell \to 1$, the transformation (14) becomes singular and the coefficient A in (24a) tends to infinity like $(\ell - 1)^{-1/2}$. Due to the restrictions of this nature, the theory is probably not very good for $\ell < 2$ and is certainly invalid for large angles of attack.

Within the range of validity $(\alpha \ll 1$ and $\ell < 2)$ of the linear

theory, a direct comparison (see Figs. 5, 6, 9, 10) between the linear and nonlinear theories shows that as a general trend the linearized solution gives larger values of lift and drag than the nonlinear solution. The discrepancy between the two solutions for the lift and drag increases with increasing angle of attack. For the flat plate, the two solutions agree very well for $\alpha = 2^{\circ}$; but the difference between the two values of C_L exceeds 17% for $\alpha > 10^{\circ}$. With the additional effects of camber the difference increases with increasing camber and σ. For $\gamma = 8^{\circ}$, the difference in C_L increases from 14% at $\alpha = 4^{\circ}$ to 30% at $\alpha = 12^{\circ}$ (see Fig. 9). Some experimental observations[6] have been carried out for some medium and large angles of attack, with which the nonlinear solution was found to be in good agreement.[1] This would imply a poorer accuracy of the linear theory in predicting experimental results, especially for hydrofoils with arbitrary camber. Thus, it seems worthwhile to carry out more experiments at small angles of attack so that a more concrete conclusion can be drawn.

As the present two solutions stand, they both indicate that C_L increases continuously with increasing σ as ℓ decreases from infinity toward unity. On the other hand, it is observed experimentally that for given α and $\eta(x)$, there is a critical cavitation number, σ_c, such that the cavity length ℓ becomes less than the chord for $\sigma > \sigma_c$. For further increase in σ, ℓ decreases to zero and C_L tends to the fully wetted (aerodynamic) value. The case of partially cavitating flow ($\ell < 1$) over a flat plate has been treated by Acosta,[7] using a similar linear theory. There it was found that the theory is limited to the values $\ell < 0.74$; beyond this range the solution also shows the singular behavior. While the nonlinear theory, also, has no way to predict the occurrence of $\ell = 1$, its result near $\ell = 1$ is apparently better than the linear theories since its singular behavior as $\ell \rightarrow 1$ is not so strong. It thus seems that to solve the problem of cavity flow with ℓ nearly equal to the chord, more detailed information and careful analysis are needed to understand the physical nature of the flow, especially near the trailing edge.

REFERENCES

1. Wu, T. Yao-tsu, "A Free Streamline Theory for Two-dimensional Fully Cavitated Hydrofoils", California Institute of Technology, Hydrodynamics Laboratory Report No. 21-17, July, 1955.

2. Tulin, M. P., "Supercavitating Flow Past Foils and Struts", paper No. 16, Symposium on Cavitation in Hydrodynamics, September, 1955, National Physical Laboratory, Teddington, England.

3. Parkin, B. R., "A Note on the Cavity Flow Past a Hydrofoil in a Liquid with Gravity", California Institute of Technology, Hydrodynamics Laboratory Report No. 47-9, 1956.

4. Biot, M. A., "Some Simplified Methods in Airfoil Theory", J. Aeronautical Sciences, Vol. 9, No. 5, 185-190, 1942.

5. Stewart, H. J., "A Simplified Two-dimensional Theory of Thin Airfoils", J. Aeronautical Sciences, Vol. 9, No. 12, 452-456, 1942.

6. Parkin, B. R., "Experiments on Circular Arc and Flat Plate Hydrofoils in Noncavitating and in Full Cavity Flow", California Institute of Technology, Hydrodynamics Laboratory Report No. 47-6, 1956.

7. Acosta, A. J., "A Note on Partial Cavitation of Flat Plate Hydrofoils", California Institute of Technology, Hydrodynamics Laboratory Report No. E-19.9, October, 1955.

APPENDIX I

Comparison of Two Systems of Perturbation Velocity

First, it may be pointed out that in several respects the linearization used in the cavitated hydrofoil problem differs slightly from that usually employed in thin airfoil theory. In the airfoil problem there is only one characteristic velocity, namely the free stream velocity U, so that, when the perturbation velocity is written as $q = U(1 + u_1, v_1)$, the linearization becomes straightforward by neglecting u_1^2, v_1^2 and higher order terms in the formulation. In the cavitated hydrofoil case, however, there are two characteristic velocities: one is U, the other is the constant velocity q_c on the cavity boundary, given by $q_c = U\sqrt{1+\sigma}$. This would imply that the use of q_c as reference for the perturbation velocity such that $q = q_c(1+u, v)$ should provide a more direct approximation of the flow quantities near the hydrofoil. Furthermore, in thin airfoil theory the parameters that are considered small are the attack angle α, the camber and thickness function; while in cavitated hydrofoil theory the small parameters are α, the camber function, and the cavitation number σ. In the latter case, the linearization is applied, in a strict sense, only to α and the camber function, while the range of validity of σ should be determined from the solution. It may turn out that these parameters are not separable so that a relative order of magnitude may not be given for them. For example, if we put $\ell = 2$ in Eq. (43), then $\sigma \cong 2\alpha$ approximately; hence in the region of validity $\ell > 2$, the quantity σ/α is not necessarily small. Thus, it seems of interest to discuss these different systems of approximation, both of which may be employed to formulate the problem of cavitated hydrofoil flows.

In the following, these two systems of perturbation velocity (u, v) and (u_1, v_1), based respectively on the reference velocity q_c and U, are discussed by comparing their corresponding boundary conditions and the resulting pressure coefficient calculations.

Reference velocity:

$$q_c = U\sqrt{1+\sigma} \qquad \Big| \qquad U \qquad (A.1)$$

Definition:

$$\vec{q}/q_c = (1+u,\ v)\ ; \qquad \vec{q}/U = (1+u_1,\ v_1)\ . \tag{A.2}$$

By comparison of the above definitions and by using the relation between q_c and U, the two systems are related by

$$u_1 = \sqrt{1+\sigma}\,(u+\beta)\ , \qquad v_1 = \sqrt{1+\sigma}\ v\ , \qquad (\beta = 1-(1+\sigma)^{-1/2})\ . \tag{A.3}$$

Now we consider their boundary conditions:
At infinity; $\vec{q} = (U, 0)$, hence

$$u_\infty = -\beta\ , \quad v_\infty = 0\ ; \qquad u_{1_\infty} = 0\ , \quad v_{1_\infty} = 0\ . \tag{A.4}$$

On the cavity boundary, $|\vec{q}| = q_c$, hence up to the linear term,

$$q_c = q_c\sqrt{(1+u)^2+v^2} \cong q_c(1+u) \qquad q_c = U\sqrt{(1+u_1)^2+v_1^2} = U(1+u_1)$$

or

$$u_c = 0\ ; \qquad u_{1_c} = (\sqrt{1+\sigma} - 1)\ . \tag{A.5}$$

On the wetted surface, which is held at a small attack angle α,

$$\frac{v}{1+u} \cong v = -\alpha\ ; \qquad \frac{v_1}{1+u_1} \cong \frac{v_1}{1+u_{1_c}} = \frac{v_1}{\sqrt{1+\sigma}} = -\alpha\ . \tag{A.6}$$

The conditions (A.4) and (A.5) are consistent with (A.3). Note, however, that in (A.6) when u is approximated by $u_c = 0$, so should u_1 be approximated by u_{1_c} in order that they agree with (A.3).

In the calculation of the pressure coefficient C_p, as defined by Eq. (12) in the text, if we neglect the nonlinear terms in the Bernoulli equation (1), then we obtain

$$p_c + \frac{1}{2}\rho q_c^2 \cong p + \frac{1}{2}\rho q_c^2 (1+2u) \qquad \left| \qquad p_c + \frac{1}{2}\rho q_c^2 \cong p + \frac{1}{2}\rho U^2 (1+2u_1) \right. \tag{A.7}$$

hence

$$C_p = \frac{p - p_c}{\frac{1}{2}\rho U^2} = -(1+\sigma)(2u) \qquad \left| \qquad C_p = \frac{p - p_c}{\frac{1}{2}\rho U^2} = \sigma - 2u_1 \right. \tag{A.8}$$

These two expressions are not consistent with (A. 3) and differ from each other by a term of the order of (σu) which is not necessarily small when $\sigma > 0.1$. Furthermore, according to condition (A. 5) the expression $C_p = -(1+\sigma)(2u)$ vanishes, and hence is continuous, at the trailing edge, as it should; while $C_p = \sigma - 2u_1$ has a jump across the trailing edge by a quantity equal to $(2+\sigma - 2\sqrt{1+\sigma})$. The explanation of this discrepancy is quite obvious because in the neglected term u_1^2 there is also a term linear in u, as can be seen from (A. 3). Thus, if the term u_1^2 is retained, then

$$p_c + \frac{1}{2}\rho q_c^2 \cong p + \frac{1}{2}\rho U^2 (1+u_1)^2$$

and hence

$$C_p \cong (1+\sigma) - (1+u_1)^2$$

which then agrees, up to the linear term of u, with $C_p = -(1+\sigma)(2u)$ according to relation (A. 3).

In view of these considerations, the reference velocity q_c is used in this report. When the reference velocity U is used, as has been done in previous investigations, an error in the linearization may occur as is shown for example in (A. 8).

APPENDIX II

Evaluation of the Integral

$$J_n = \frac{1}{\pi}\int_0^{\pi} \frac{\cos n\theta}{a^2 + \cos^4\frac{\theta}{2}}\, d\theta , \qquad \begin{pmatrix} a \text{ being real, } > 0 \\ \text{and } n = 0, 1, 2, \ldots \end{pmatrix} .$$

First, this integral may be written as

$$J_n = \frac{2}{\pi}\int_0^{2\pi} \frac{\cos n\theta}{(\cos\theta - b)(\cos\theta - \bar{b})}\, d\theta = \frac{4}{\pi}\, R\ell\frac{1}{b - \bar{b}}\int_0^{2\pi} \frac{\cos n\theta}{\cos\theta - b}\, d\theta ,$$

with

$$b = -(1 + 2ai) , \qquad i = \sqrt{-1} .$$

Upon transformation of the variable $z = e^{i\theta}$, one obtains

$$J_n = \frac{1}{\pi a}\, R\ell \oint \frac{(z^n + z^{-n})}{(z - \zeta)(z - \zeta^{-1})}\, dz$$

where the closed contour is $|z| = 1$ and

$$\zeta = b + \sqrt{b^2 - 1} , \qquad \zeta^{-1} = b - \sqrt{b^2 - 1} .$$

Inside the contour the integrand has a simple pole at $z = \zeta^{-1}$ and a pole of order n at the origin, while the pole $z = \zeta$ is outside the contour for $a > 0$. The residue at $z = \zeta^{-1}$ is $(\zeta^n + \zeta^{-n})/(\zeta^{-1} - \zeta)$ and the residue at $z = 0$ is $(\zeta^n - \zeta^{-n})/(\zeta - \zeta^{-1})$. Hence

$$J_n = -\frac{4}{a}\, R\ell\left\{\frac{i\,\zeta^{-n}}{\zeta - \zeta^{-1}}\right\} = \frac{2}{a}\, R\ell\left\{\frac{(b - \sqrt{b^2 - 1})^n}{i\sqrt{b^2 - 1}}\right\}$$

But from Eqs. (22) and (23),

$$\sqrt{b^2-1} = 2\sqrt{(-ia)(-ia-1)} = \sqrt{a}\,(1-i)(\epsilon-i\delta)\,, \qquad b-\sqrt{b^2-1} = \lambda+i\tau\,.$$

Therefore,

$$J_n = R\ell\,\frac{\left[(\delta+\epsilon)+i(\delta-\epsilon)\right]\left[\lambda+i\tau\right]^n}{2a^{3/2}(1+a^2)^{1/2}}\,.$$

ACKNOWLEDGMENT

The author wishes to express his appreciation to Professor M. S. Plesset and Dr. B. R. Parkin for many helpful discussions. He is also grateful to Mrs. Rose Grant for her assistance in the preparation of the report.

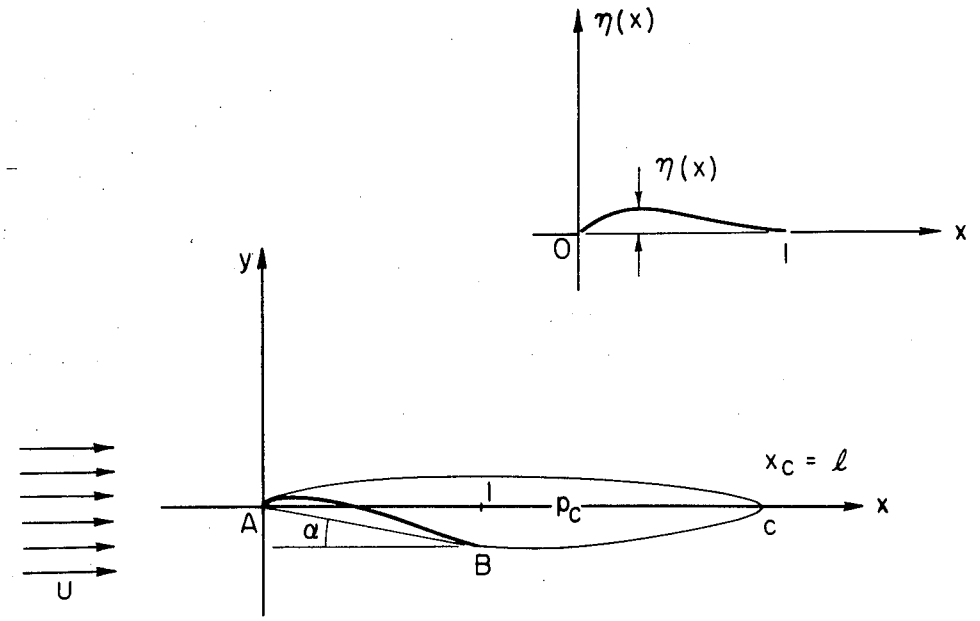

Fig. 1 - A typical flow configuration.

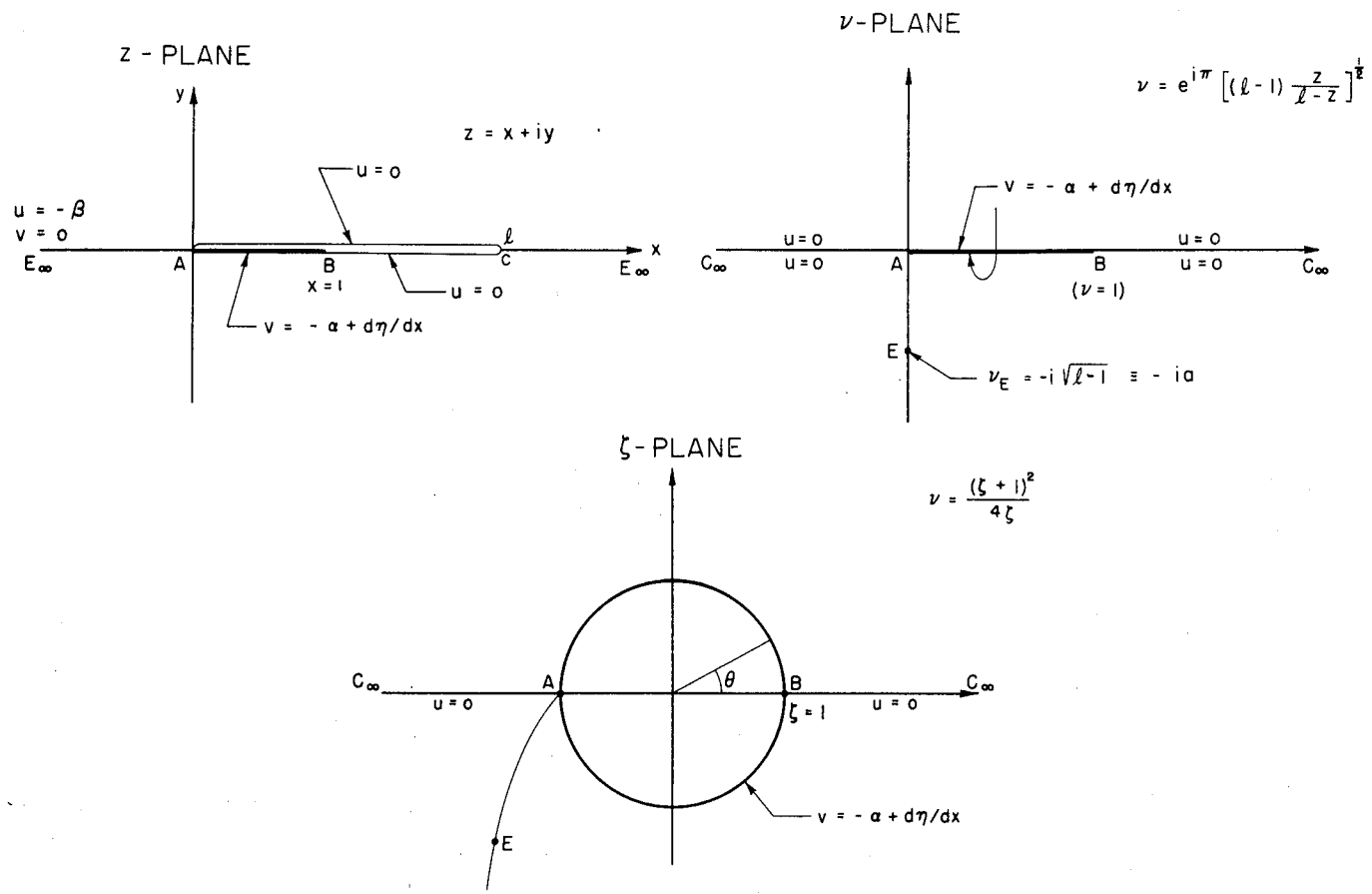

Fig. 2 - Linearized boundary conditions and their conformal transformations.

$$\sqrt{b^2-1} = 2\sqrt{(-ia)(-ia-1)} = \sqrt{a}\,(1-i)(\epsilon - i\delta)\,, \qquad b - \sqrt{b^2-1} = \lambda + i\tau\,.$$

Therefore,

$$J_n = R\ell\,\frac{\left[(\delta+\epsilon)+i(\delta-\epsilon)\right]\left[\lambda+i\tau\right]^n}{2a^{3/2}(1+a^2)^{1/2}}\,.$$

ACKNOWLEDGMENT

The author wishes to express his appreciation to Professor M. S. Plesset and Dr. B. R. Parkin for many helpful discussions. He is also grateful to Mrs. Rose Grant for her assistance in the preparation of the report.

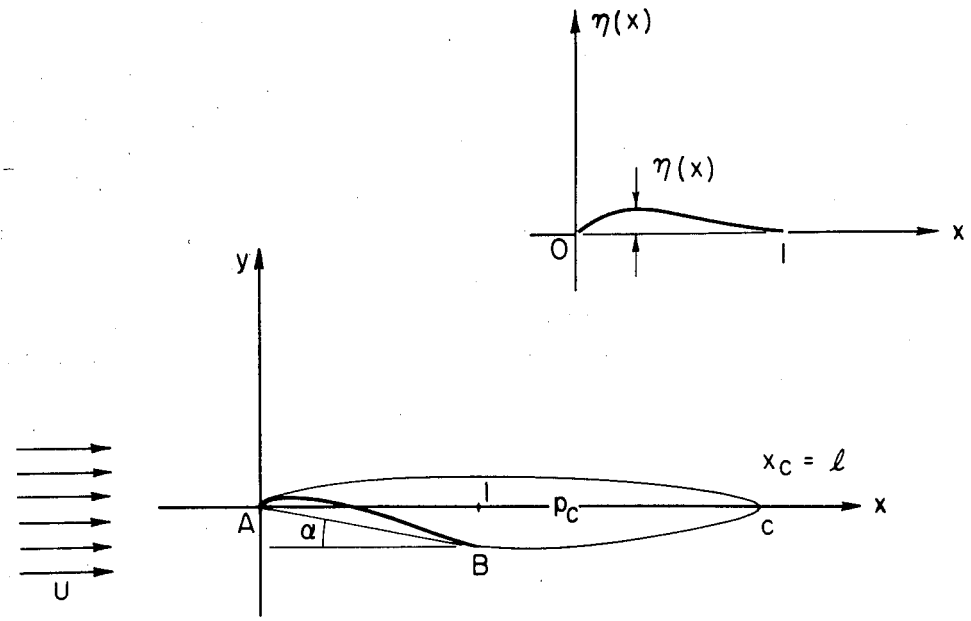

Fig. 1 - A typical flow configuration.

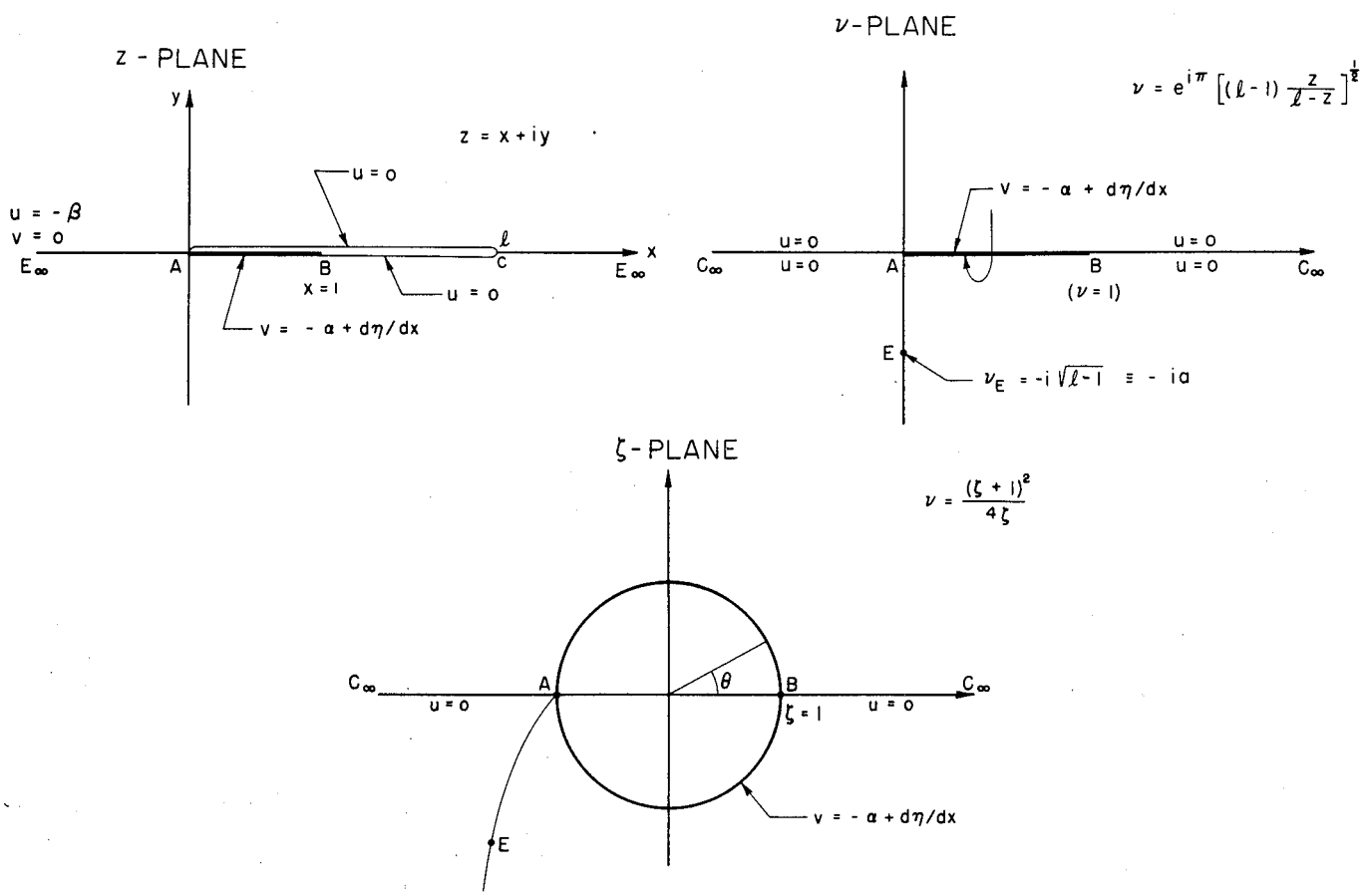

Fig. 2 - Linearized boundary conditions and their conformal transformations.

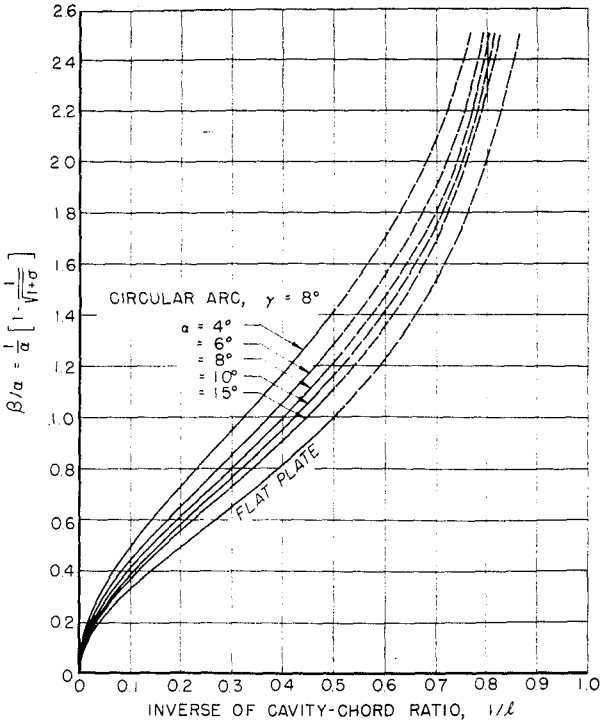

Fig. 3 - Cavity length ℓ in terms of σ and α.

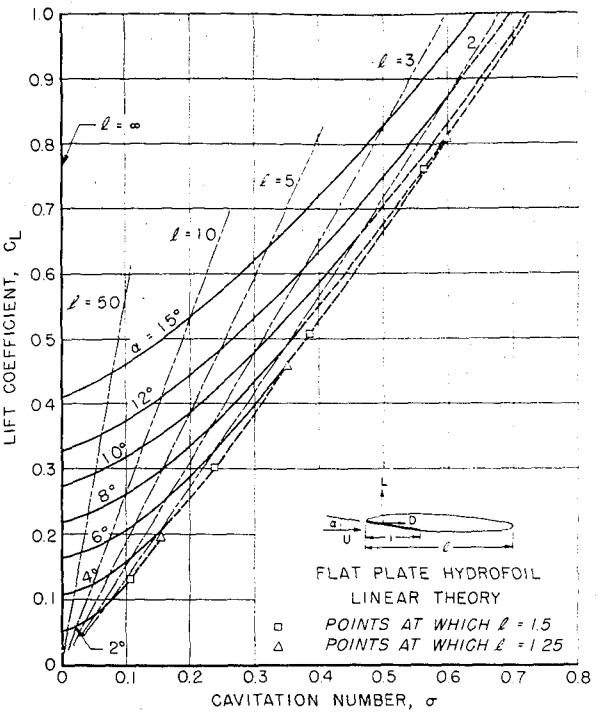

Fig. 4 - Effect of σ on C_L for flat plate hydrofoil (linear theory).

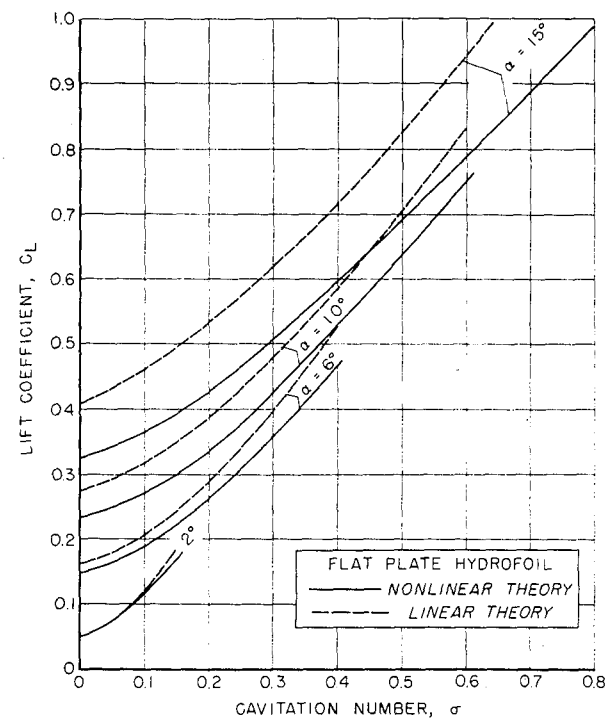

Fig. 5 - Comparison of the linear and nonlinear theories for C_L.

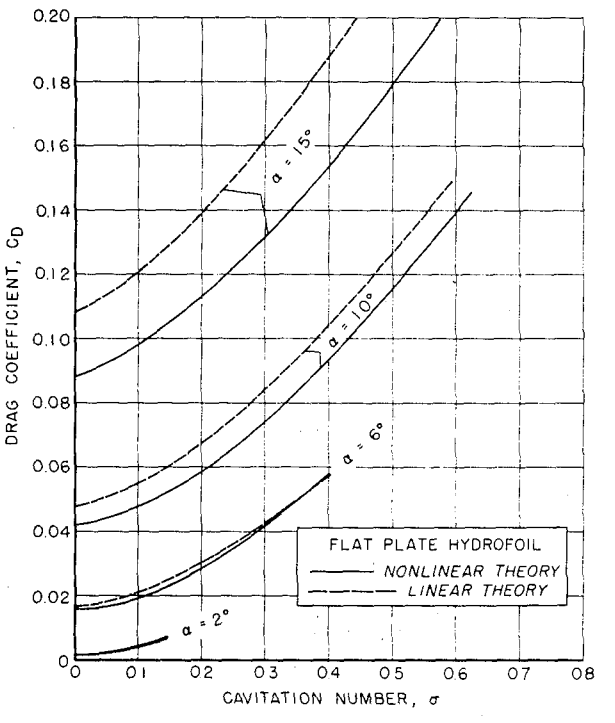

Fig. 6 - Comparison of the linear and nonlinear theories for C_D.

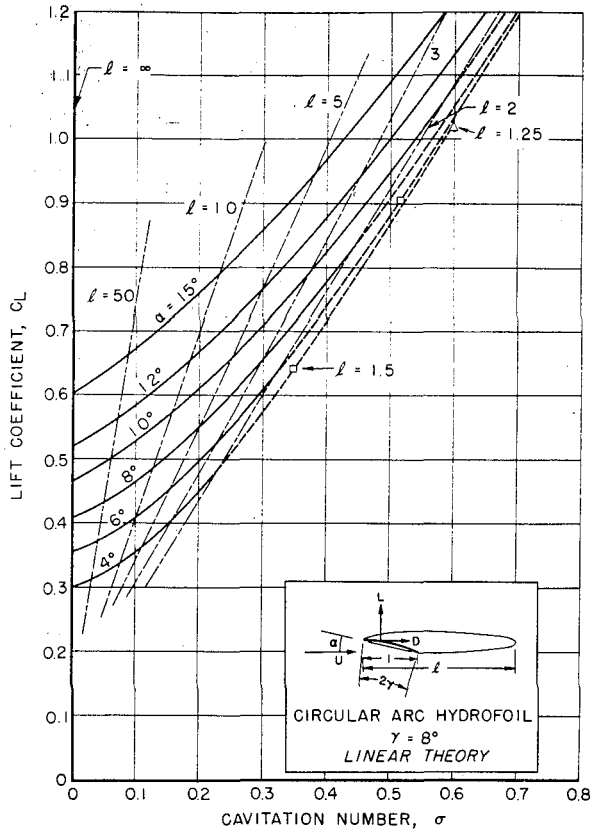

Fig. 7 - Effect of σ on C_L for the circular arc hydrofoil (linear theory).

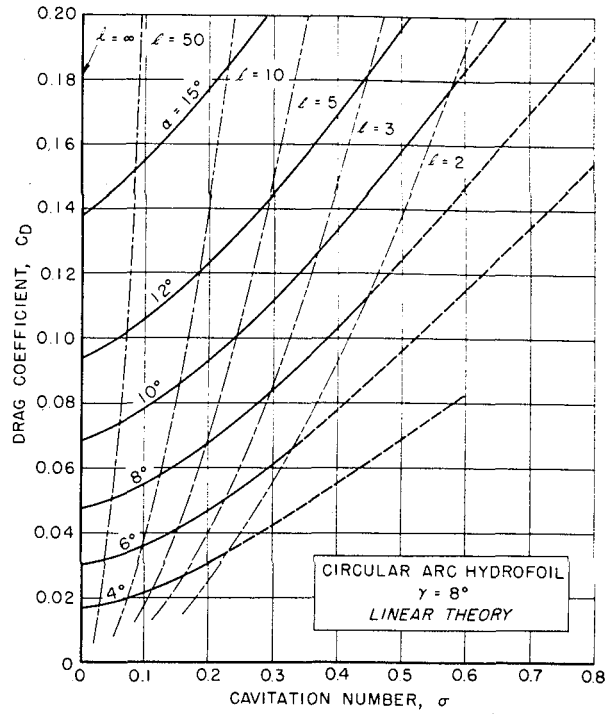

Fig. 8 - Effect of σ on C_D for the circular arc hydrofoil (linear theory).

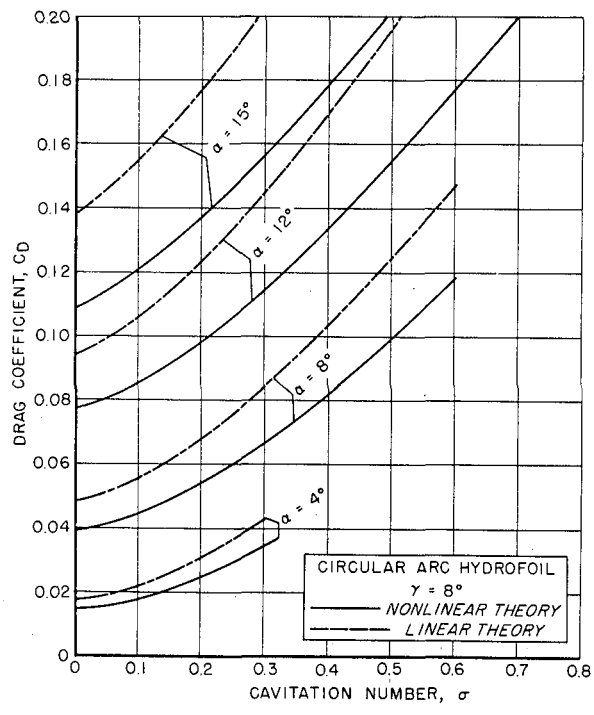

Fig. 9 - Comparison of the linear and nonlinear theories for C_L.

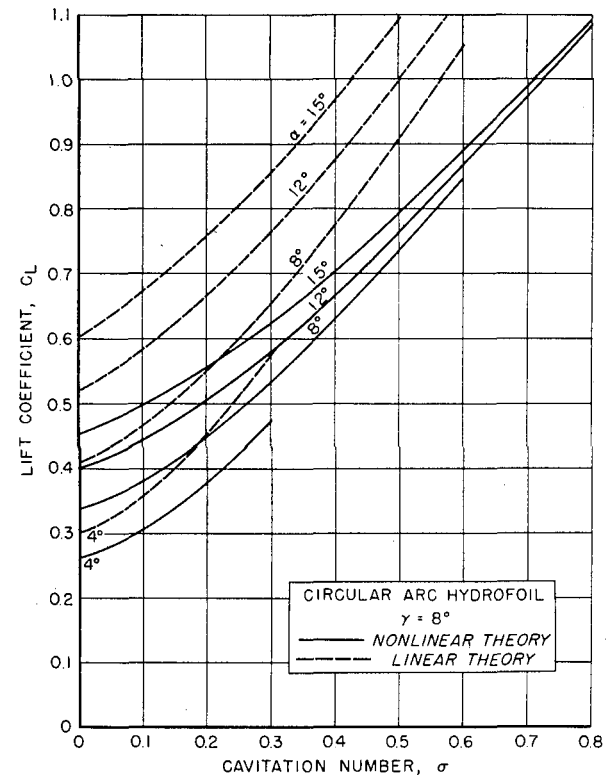

Fig. 10 - Comparison of the linear and nonlinear theories for C_D.

DISTRIBUTION LIST FOR UNCLASSIFIED
REPORTS ON CAVITATION
Contract N6onr-24420 (NR 062-059)

Chief of Naval Research
Navy Department
Washington 25, D. C.
Attn: Code 438 (3)
Code 463 (1)

Commanding Officer
Office of Naval Research
Branch Office
The John Crear Library Bldg.
86 E. Randolph Street
Chicago 1, Illinois (1)

Commanding Officer
Office of Naval Research
Branch Office
346 Broadway
New York 13, New York (1)

Commanding Officer
Office of Naval Research
Branch Office
1030 East Green Street
Pasadena 1, California (1)

Commanding Officer
Office of Naval Research
Navy 100, Fleet Post Office
New York, New York (25)

Director
Naval Research Laboratory
Washington 25, D. C.
Attn: Code 2021 (6)

Chief, Bureau of Aeronautics
Navy Department
Washington 25, D. C.
Attn: Research Division (1)
Aero and Hydro Branch
(Code Ad-3) (1)
Appl. Mech. Branch
(Code DE-3) (1)

Chief, Bureau of Ordnance
Navy Department
Washington 25, D. C.
Attn: Asst. Chief for Research
(Code Re) (1)
Systems Director, Underwater Ord (Code Rexc) (1)
Armor, Bomb, Projectile, Rocket, Guided Missile Warhead and Ballistics Branch
(Code Re3) (1)
Torpedo Branch (Code Re6) (1)
Research and Components Section (Code Re6a) (1)
Mine Branch (Code Re7) (1)

Chief, Bureau of Ships
Navy Department
Washington 25, D. C.
Attn: Research and Development (Code 300) (1)
Ship Design (Code 410) (1)
Preliminary Design and Ship Protection (Code 420) (1)
Scientific, Structural and Hydrodynamics (Code 442) (1)
Submarines (Code 525) (1)
Propellers and Shafting
(Code 554) (1)

Chief, Bureau of Yards and Docks, Navy Department
Washington 25, D. C.
Attn: Research Division (1)

Commander
Naval Ordnance Test Station
3202 E. Foothill Blvd.
Pasadena, California
Attn: Head, Underwater Ord. (1)
Head, Research Div. (1)

Commander
Naval Ordnance Test Station
Inyokern, China Lake, Calif.
Attn: Technical Library (1)

Commanding Officer and Director
David Taylor Model Basin
Washington 7, D.C.
Attn: Hydromechanics Lab. (1)
Seaworthiness and Fluid Dynamics Div. (1)
Library (1)

Commanding Officer
Naval Ordnance Laboratory
White Oak, Maryland
Attn: Underwater Ord. Dept. (1)

Commanding Officer
Naval Underwater Ordnance Sta.
Newport, Rhode Island (1)

Director
Underwater Sound Laboratory
Fort Trumbull
New London, Connecticut (1)

Librarian
U.S. Naval Postgraduate School
Monterey, California (1)

Executive Secretary
Research and Development Board
Department of Defense
The Pentagon
Washington 25, D.C. (1)

Chairman
Underseas Warfare Committee
National Research Council
2101 Constitution Avenue
Washington 25, D.C. (1)

Dr. J. H. McMillen
National Science Foundation
1520 H Street, N.W.
Washington, D.C. (1)

Director
National Bureau of Standards
Washington 25, D.C.
Attn: Fluid Mechanics Section (1)

Dr. G. H. Keulegan
National Hydraulic Laboratory
National Bureau of Standards
Washington 25, D.C. (1)

Director of Research
National Advisory Committee for Aeronautics
1512 H Street, N.W.
Washington 25, D.C. (1)

Director
Langley Aeronautical Laboratory
National Advisory Committee for Aeronautics
Langley Field, Virginia (1)

Mr. J. B. Parkinson
Langley Aeronautical Laboratory
National Advisory Committee for Aeronautics
Langley Field, Virginia (1)

Commander
Air Research and Development Command
P.O. Box 1395
Baltimore 18, Maryland
Attn: Fluid Mechanics Div. (1)

Director
Waterways Experiment Station
Box 631
Vicksburg, Mississippi (1)

Beach Erosion Board
U.S. Army Corps of Engineers
Washington 25, D.C. (1)

Office of Ordnance Research
Department of the Army
Washington 25, D.C. (1)

Office of the Chief of Engineers
Department of the Army
Gravelly Point
Washington 25, D.C. (1)

Commissioner
Bureau of Reclamation
Washington 25, D.C. (1)

Director
Oak Ridge National Laboratory
P.O. Box P
Oak Ridge, Tennessee (1)

Director
Applied Physics Division
Sandia Laboratory
Albuquerque, New Mexico (1)

Professor Carl Eckart
Scripps Institute of Oceanography
La Jolla, California (1)

Documents Service Center
Armed Services Technical
Information Agency
Knott Building
Dayton 2, Ohio (5)

Office of Technical Services
Department of Commerce
Washington 25, D.C. (1)

Polytechnic Institute of Brooklyn
Department of Aeronautical
Engineering and Applied Mech.
99 Livingston Street
Brooklyn 1, New York
Attn: Prof. H. Reissner (1)

Division of Applied Mathematics
Brown University
Providence 12, Rhode Island (1)

California Institute of Technology
Pasadena 4, California
Attn: Hydrodynamics Laboratory
Professor A. Hollander (1)
Professor R. T. Knapp (1)
Professor M. S. Plesset (1)
Professor V. A. Vanoni (1)
GALCIT
Prof. C.B. Millikan, Director (1)
Prof. Harold Wayland (1)

University of California
Berkeley 4, California
Attn: Professor H.A. Einstein
Dept. of Engineering (1)
Professor H. A. Schade,
Dir. of Engr. Research (1)

Case Institute of Technology
Department of Mechanical Engineering
Cleveland, Ohio
Attn: Professor G. Kuerti (1)

Cornell University
Graduate School of Aeronautical
Engineering
Ithaca, New York
Attn: Prof. W.R. Sears, Director(1)

Harvard University
Dept. of Mathematics
Cambridge 38, Mass.
Attn: Prof. G. Birkhoff (1)

University of Illinois
Dept. of Theoretical and
Applied Mechanics
College of Engineering
Urbana, Illinois
Attn: Dr. J. M. Robertson (1)

Indiana University
Dept. of Mathematics
Bloomington, Indiana
Attn: Professor D. Gilbarg (1)

State University of Iowa
Iowa Institute of Hydraulic
Research, Iowa City, Iowa
Attn: Dr. Hunter Rouse, Dir. (1)

University of Maryland
Inst. for Fluid Dynamics and
Applied Mathematics
College Park, Maryland
Attn: Prof. M. H. Martin,
Director (1)
Prof. J. R. Weske (1)

Massachusetts Institute of
Technology
Cambridge 39, Mass.
Attn: Prof. W.M. Rohsenow,
Dept. Mech. Engr. (1)
Prof. A.T. Ippen,
Hydrodynamics Laboratory (1)

Michigan State College
Hydraulics Laboratory
East Lansing, Michigan
Attn: Prof. H.R. Henry (1)

University of Michigan
Ann Arbor, Michigan
Attn: Director, Engineering
Research Institute (1)
Prof. V.L. Streeter,
Civil Engineering Dept. (1)

University of Minnesota
St. Anthony Falls Hydraulic Lab.
Minneapolis 14, Minnesota
Attn: Dr. L.G. Straub, Dir. (1)

New York University
Institute of Mathematical Sciences
25 Waverly Place
New York 3, New York
Attn: Prof. R. Courant, Dir. (1)

University of Notre Dame
College of Engineering
Notre Dame, Indiana
Attn: Dean K.E. Schoenherr (1)

Pennsylvania State University
Ordnance Research Laboratory
University Park, Pennsylvania
Attn: Prof. G.F. Wislicenus (1)

Rensselaer Polytechnic Inst.
Dept. of Mathematics
Troy, New York
Attn: Dr. Hirsh Cohen (1)

Stanford University
Stanford, California
Attn: Applied Math. and
Statistics Laboratory (1)
Prof. P.R. Garabedian (1)
Prof. L.I. Schiff, Dept. of
Physics (1)
Prof. J.K. Vennard, Dept.
of Civil Engineering (1)

Stevens Institute of Technology
Experimental Towing Tank
711 Hudson Street
Hoboken, New Jersey (1)

Worcester Polytechnic Institute
Alden Hydraulic Laboratory
Worcester, Mass.
Attn: Prof. J.L. Hooper,
Director (1)

Dr. Th. von Karman
1051 S. Marengo Street
Pasadena, California (1)

Aerojet General Corporation
6352 N. Irwindale Avenue
Azusa, California
Attn: Mr. C. A. Gongwer (1)

Dr. J.J. Stoker
New York University
Institute of Mathematical Sciences
25 Waverly Place
New York 3, New York (1)

Prof. C.C. Lin
Dept. of Mathematics
Massachusetts Institute of
Technology
Cambridge 39, Mass. (1)

Dr. Columbus Iselin
Woods Hole Oceanographic Inst.
Woods Hole, Mass. (1)

Dr. A.B. Kinzel, Pres.
Union Carbide and Carbon Re-
search Laboratories, Inc.
30 E. 42nd St.
New York, N.Y. (1)

Dr. F.E. Fox
Catholic University
Washington 17, D.C. (1)

Dr. Immanuel Estermann
Office of Naval Research
Code 419
Navy Department
Washington 25, D.C. (1)

Goodyear Aircraft Corp.
Akron 15, Ohio
Attn: Security Officer (1)

Dr. F.V. Hunt
Director Acoustics Research
Laboratory
Harvard University
Cambridge, Mass. (1)

Prof. Robert Leonard
Dept. of Physics
University of California at
Los Angeles
West Los Angeles, Calif. (1)

Prof. R.E.H. Rasmussen
Buddenvej 47, Lyngby
Copenhagen, Denmark
via: ONR, Pasadena, Calif. (1)

Technical Librarian
AVCO Manufacturing Corp.
2385 Revere Beach Parkway
Everett 49, Mass. (1)

Dr. L. Landweber
Iowa Inst. of Hydraulic Research
State University of Iowa
Iowa City, Iowa (1)